Eur. Phys. J. B **27**, 167–172 (2002)
DOI: 10.1140/epjb/e20020142

THE EUROPEAN PHYSICAL JOURNAL B
EDP Sciences

Hydrodynamics and cell motion during the rounding of two dimensional hydra cell aggregates

J.-P. Rieu[1,a] and Y. Sawada[2]

[1] Département de Physique des Matériaux, Université Claude Bernard – Lyon I, 43 boulevard du 11 Novembre 1918, 69622 Villeurbanne Cedex, France
[2] Tohoku Institute of Technology Yagiyama-Kasumi, Taihaku, 983, Sendai, Japan

Received 21 December 2001

Abstract. Using a two dimensional experimental geometry, we study hydrodynamics and cell motion during the rounding-up of three kinds of *hydra* aggregates (ectodermal, endodermal and mixed). The relaxation of initially elongated aggregates toward a circular shape is exponential and the relaxation time is proportional to the aggregate size as expected from hydrodynamics laws. As for viscous liquids, aggregate rounding is driven by tissue surface tensions σ and resisted by tissue viscosity η. The ratio η/σ is the same for the three kinds of aggregates. With a reasonable value $\sigma = 1$ mN/m, we obtain an estimate larger than 10^4 Pa s for the tissue viscosity. Cell motion during rounding is strongly cooperative and cell displacements exhibit some specific patterns in each aggregate. These results point out the role of adhesive bonds in the observed kinetics.

PACS. 87.18.Ed Aggregation and other collective behavior of motile cells – 87.17.Jj Cell locomotion; chemotaxis and related directed motion – 87.19.Tt Rheology of body fluids

1 Introduction

It is now well established that certain living tissues mimic the behavior of viscous liquids [1]. When multiple types of cells from a primitive animal or an embryo are dissociated, randomly intermingled and then reaggregated, they are able to rearrange, to re-establish coherent homotypic domains. This rearrangement of cells, known as cell sorting, is analogous to the demixing of immiscible liquids. The fusion or the rounding up of cell populations are also similar to the coalescence or rounding up of liquid droplets: these processes are driven by tissue surface tensions σ and resisted by tissue viscosity η [2].

Steinberg first proposed that cell sorting is driven by surface energy minimization [3]. Its differential adhesion hypothesis (DAH) postulates that tissues possess interfacial tensions arising from the adhesive interactions between individual cells, and predicts that mixed populations of sufficiently mobile cells rearrange so that the less cohesive cells envelop the more cohesive cells [4]. The surface tensions of different chicken embryonic tissues have been measured using a parallel plate compression apparatus [5]. The relative magnitudes of these tensions predict correctly the mutual envelopment of these tissues [6]. The analysis of the relaxation of embryonic aggregates subjected to mechanical deformations, either by centrifugation [7] or by compression [8], demonstrated that tissues relax as elastic materials on short time scales and as viscous liquids on long time scales. The relaxation of compressed cellular aggregates was analyzed using a kelvin model of viscoelasticity [8]. As stated by the authors, this model may represent a strong oversimplification of the tissue rheology but it gives an estimation of the tissue elastic and viscous parameters [8]. Earlier, Gordon *et al.* obtained quantitative values of the ratio η/σ from the hydrodynamical analysis of the fusion and the rounding of cellular aggregates [2]. However, the authors gave only orders of magnitude of this parameter as they performed only preliminary experiments, presumably because it was difficult to obtain suspended three dimensional aggregates which were fixed over long times (rotation or flattening on a surface are undesirable).

In this work, we show that the hydrodynamical laws also apply for the rounding-up of two dimensional (2D) aggregates of mixed ectodermal and endodermal *hydra* cells in various proportions. This 2D system is interesting because it allows to track single endodermal cell motion in the same time as measuring the shape relaxation. We analyze the relaxation with the 2D hydrodynamical equations derived by Mann *et al.* for polymer monolayers in the case of dissipation dominated by surface viscosity [9]. This method allows a direct estimation of the ratio of η/σ.

[a] e-mail: rieu@dpm.univ-lyon1.fr

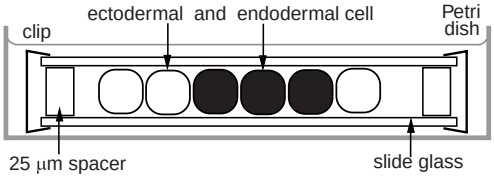

Fig. 1. 2D experimental set-up used to study aggregate shape relaxation and cell motion.

2 Experimental observations

We first study the shape relaxation of 2D *hydra* aggregates prepared according to previously reported methods [10,11]. Briefly, we dissociated and reaggregated cells and gently sandwiched them between glass slides separated by 25 μm spacers. The experimental system and the sequence of events in three kinds of aggregates are displayed in Figures 1 and 2.

Figure 2a–c corresponds to an aggregate with roughly equal proportions of each cell type. Initially, the population of endodermal cells (dark cells) consists both of single cells and clusters of several cells which are surrounded by a continuous mass of ectodermal cells (light). The aggregate is elongated. After 1 h, the aggregate slightly rounded, internal clusters grow by fusing with one another and with single cells (Fig. 2b). Rounding up is complete after 6 hours and sorting almost complete although the inner endodermal cluster is not very compact (Fig. 2c). Dead cells appear at the periphery of the aggregate, they can be distinguished from living cells by their larger size and circular shape. Later, the 2D sample slowly disaggregates [10]. In 3D, from a mixture of dissociated cells, the aggregate develops an internal cavity within 20 hours [12] and within one week a normal *hydra* might regenerate [13]. *Hydra* has indeed a strong regenerative capacity.

In Figure 2d–f, an initially elliptical pure endodermal aggregate was prepared by separating endodermal and ectodermal tissues [14]. Rounding up is completed after 6h (Fig. 2f). After that time, cell perform a random motion within the rounded aggregate during still 3h.

The aggregate displayed in Figure 2g–i was prepared by first separating tissues, putting them into contact before sandwiching the resulting aggregate between glass slides. Initially, we wanted to study the process of tissue engulfment in 2D [14], however we always obtained an initial situation under the microscope with the endodermal cells were completely surrounded by the ectodermal cluster (Fig. 2g). At that initial time ($t = 0$ h) the aggregate displays an irregular shape and the endodermal cluster is elongated. After 2h (Fig. 2h), both the full aggregate and the internal endodermal cluster have been rounding. After 7h (Fig. 2i), the inner cluster becomes circular but the external aggregate boundary seems to slightly oscillate around the circular shape. We observed frequently pure ectodermal aggregates which did not round completely during the survival of the aggregate.

3 Aggregate shape relaxation analysis

Experiments are digitized at intervals of $5 \sim 10$ min and analyzed on a computer using NIH Image [15]. We do not take into account dead cells for calculating the boundary and shape of the aggregate. These are generally loose and brighter than the living cells, they can be removed from the binarized images by a set of basic filtering operations (successive erode and dilate filters and finally thresholding). We use NIH Image for those operations and also for fitting each time the shape of the aggregate by an ellipse. We keep as the only parameter defining the aggregate deformation $d = \frac{M}{m} - 1$ where M and m are the major and minor axis of the fitted ellipse. d is zero for a perfect circle and increases for elongated aggregates.

Figure 3 shows a log-linear plot of the time dependence of the deformation of the aggregates displayed in Figure 2. We present only the internal cluster relaxation for Figure 2g–i. The ectodermal relaxation data correspond to an other aggregate not displayed in Figure 2. For each aggregate, d decreases exponentially with time. The same kind of exponential relaxation was found experimentally in the case of the 2D relaxation of polymer domains at the air/water interface by Mann *et al.* [9]. The authors showed that such exponential behavior is expected theoretically from the hydrodynamics laws. They showed also that the relaxation time T_c is either proportional to $\eta_S R/\lambda$ in case of viscosity dominated by the surface viscosity η_S where λ is the domain line tension, and R is the domain radius, either to $\eta_B R^2/\lambda$ in case of viscosity dominated by the bulk water viscosity η_B (water underneath the polymer monolayer). In case of cellular aggregates, the relaxation is driven by tissue surface tensions σ (aggregate/external medium surface tension), it is resisted by the tissue viscosity (due cell-cell adhesive bonds). About 30 years ago, Gordon *et al.* [2] found also an exponential relation for the relaxation of 3D ellipsoid of revolution into a sphere with a relaxation time scaling with the characteristic aggregate size $v^{1/3}$ where v is the volume.

In our case, the aggregate may be considered as purely two dimensional. The 2D shape relaxation is then described by a surface viscosity η_S exactly as in case of the relaxation of polymer domains at the air/water interface [9]. Furthermore, we believe the microscopic origin of this viscosity is friction between adjacent cells due to adhesive bonds, not friction at the cell-glass interface. We indeed tryed to reduce the cell/substrate adhesion by covering the glass with Albumin but we did not observe any change in the time course of cell sorting [10]. Hence, the surface viscosity is proportional to the aggregate thickness $\eta_S = \eta \times e$ [16], where η is a bulk viscosity proportional to the 3D tissue viscosity η_T. Indeed, if we model the cells within the 2D aggregate as cubes (Fig. 1), and if we assume the viscosity is proportional to the adjacent cell/cell contact area, then the surface contact between adjacent cubes in the monolayer gives $\eta = \frac{4}{6}\eta_T$. This picture of viscosity is of course oversimplified but there are no 3D measurements for comparison, then for the following we will call η the tissue viscosity. Lastly, although the concept of tissue surface σ tension was only demonstrated

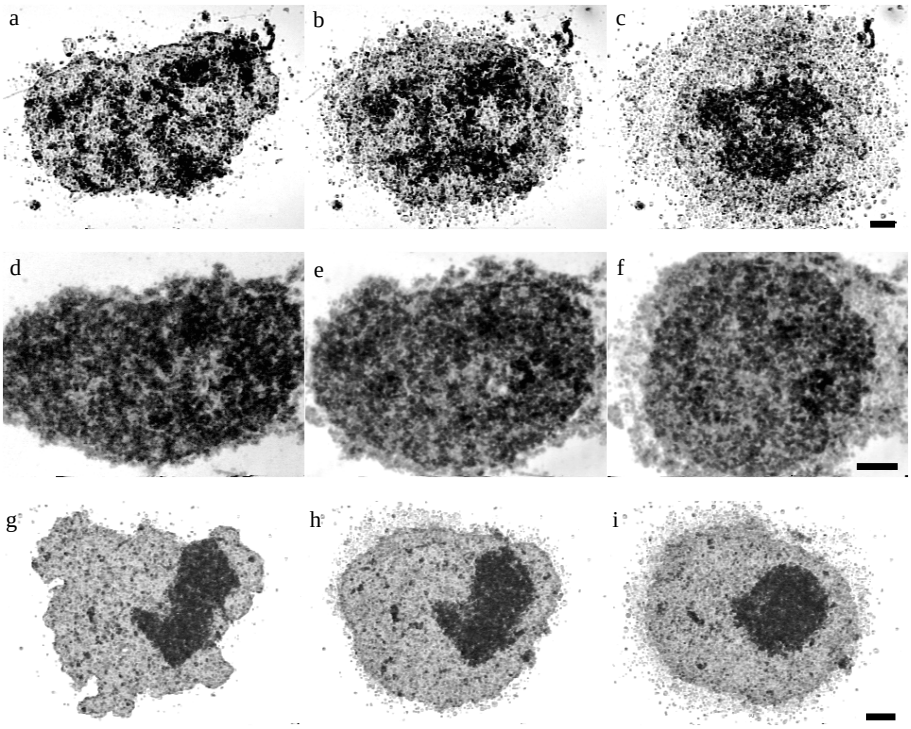

Fig. 2. Shape relaxation in 2D *hydra* aggregates. (a–c), Aggregate with nearly equal proportions of endodermal (dark) and ectodermal cells (light) at 0h (a), 1h (b) and 6h (c); bar, 50 μm. (d–e), Pure endodermal aggregate at 0h (d), 1h (e) and 6h (f); bar, 100 μm. (g–i), Aggregate with one endodermal aggregate surrounded by mostly ectodermal cells at 0h (g), 2h (h) and 7h (i); bar, 100 μm.

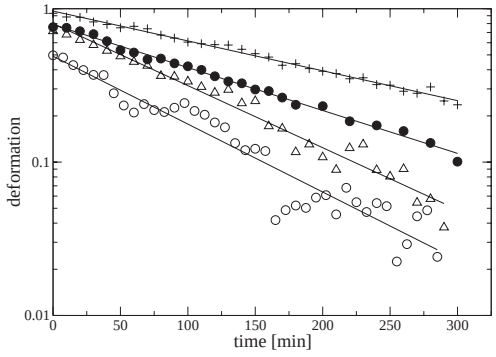

Fig. 3. Deformation parameter (see text) as a function of time for internal endodermal cluster within an ectodermal aggregate (crosses), pure endodermal aggregate (bullets), mixed aggregate (open triangles) and pure ectodermal aggregate (circles).

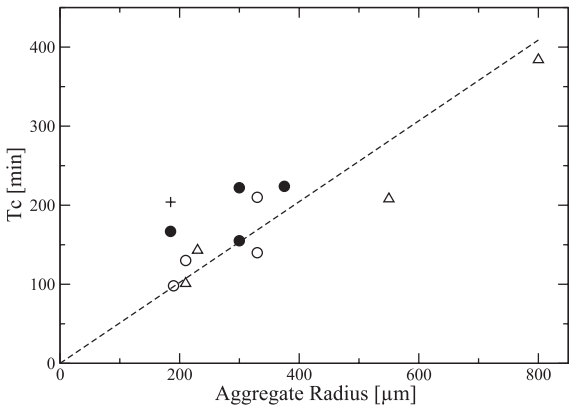

Fig. 4. Relaxation time T_c as a function of aggregate size; same legend as Figure 3.

recently using the compression plate apparatus on 3D aggregates [5], we will assume that the tissue line tension which drive the 2D relaxation is proportional to σ, *i.e.* $\lambda = \sigma \times e$. We obtain finally:

$$T_c = \frac{\eta}{\sigma} R. \qquad (1)$$

In Figure 4, we have plotted the measured relaxation time T_c of the whole experiments analyzed as a function of the aggregate size R (radius of the rounded aggregates at the end of the relaxation process). For each aggregate type, T_c is increasing with R but the scattering of the experimental points do not allow to conclude definitely on a linear increase especially for endodermal and ectodermal aggregates. It seems there are no significant differences between different aggregates. Thus we fitted the whole data (except the internal cluster data point) with equation (1). We obtained $\eta/\sigma = 0.5 \pm 0.2$ min/μm which gives $\eta = 3 \times 10^4$ Pa s (1 Pa s = 10 Poise) using $\sigma = 1$ mN/m as a typical value of tissue surface tension [5,8]. This is

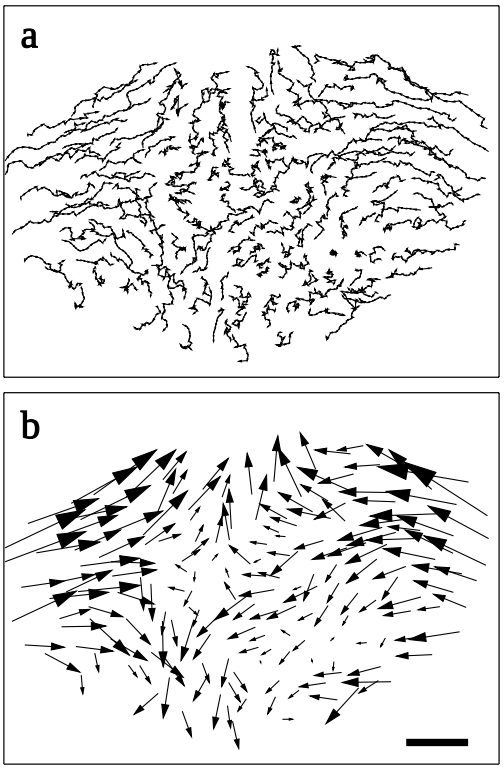

Fig. 5. (a) Cell trajectories of 184 endodermal cells in a pure endodermal aggregate; positions are reported at intervals of 10 min between 0 h and 6 h. (b) Cell displacements in the same aggregate during time interval 0–3 h; arrow size is proportional to cell displacement; bar, 100 μm.

10^7 times higher than the water viscosity. It seems that the relaxation time of the only internal endodermal cluster which could be analyzed (Fig. 2g–i) is larger than the relaxation of full aggregates of the same size. This is also expected from the hydrodynamics as the viscosity which has to be taken into account in equation (1) is in fact the sum of the viscosities inside and outside the rounding boundary [9]. Thus, for the rounding of full aggregates, external viscosity of medium (*i.e.* approximately the water viscosity) is negligible, while for the endodermal cluster, the external medium is the ectodermal aggregate which is presumably of the same order of magnitude than endodermal viscosity.

4 Individual cell motion during aggregate rounding

Using previous methods [10], we have tracked the displacements of endodermal cells during the rounding of 2D aggregates. We show two examples of such tracking in Figure 5 (184 endodermal cells in an endodermal aggregate) and Figure 6 (117 endodermal cells in a mainly ectodermal aggregate). At short times, cells present zigzag trajectories due to the random forces exerted by the surrounding

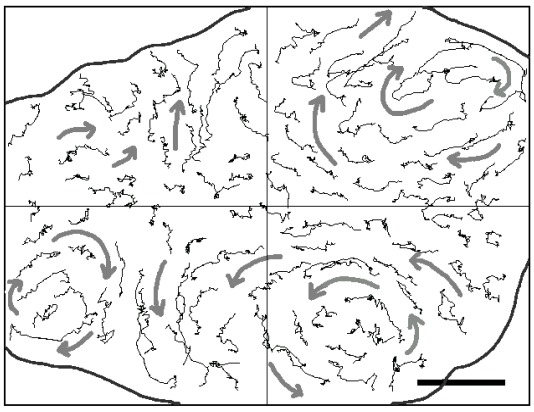

Fig. 6. Cell trajectories of 117 endodermal cells in an ectodermal aggregate; positions are reported at intervals of 10 min between 0 h and 9 h; arrows indicate the direction of cell flows; bar, 100 μm.

cells (Figs. 5a and 6). Over larger times, cells move locally in the same direction, as coherent groups. Displacements exhibit both long time and long distance correlations as previously shown during cell sorting [10]. In the endodermal aggregate, the flows describe an almost perfect saddle pattern (Fig. 5b). Rounding is achieved in about 4 hours. During the 5 following hours of aggregate survival, cells describe random trajectories (not shown). We calculated the mean cell velocity and found it is faster at the very beginning of the rounding. Then it slows down progressively and then remains constant once rounding is completed. During the rounding of less symmetric endodermal aggregates, we observed less symmetric displacement patterns but motion was also coherent. In case of ectodermal aggregate, we sometimes do not observe complete rounding as in Figure 6. Here, circular flows organize in at last three part of the aggregate. By looking the time-lapse recording of this experiment, these flows suddenly appeared after 200 min as if they were triggered by some instability. The apparition of these flows coincide with a peak in the mean cell velocity. We also observed circular flows in an other pure ectodermal aggregate, never in endodermal aggregates. They do not seem to help the rounding process.

5 Discussion

As predicted by hydrodynamics, the shape relaxation of 2D *hydra* cell aggregates is exponential and the relaxation time seems to scale with the aggregate radius. The analysis of 2D shape relaxation allows thus to estimate the ratio of tissue viscosity over tissue surface tension. In order to obtain separately these quantities, it is necessary to complete these observations with an other technique. Direct measurements of tissue viscosity have never been performed to our best knowledge. It will be interesting to use a surface viscosimeter [16] or to measure the drag force exerted on a moving disk within the 2D layer [17]. On the other hand, tissue surface tension are measured using the compression plate apparatus of Foty *et al.* The method lies

on the analysis of the equilibrium shape of compressed aggregates using Laplace's equation. This apparatus allows also to study the relaxation of 3D aggregates [8]. In principle, if the cells within the compressed aggregate equilibrated their shape [7], it should be possible after the release of the compression to analyze the shape relaxation of this roughly oblate ellipsoid with the equation established for the rounding of an ellipsoid of revolution [2]. This is valid for not too compressed aggregates. An other simple geometry for which the hydrodynamics equations have been solved is the fusion of two identical spherical drops of viscous liquid. When placed in contact, the drops fuse together. The beginning of such fusion as a function of time t is described by

$$x^2 = \frac{3R\sigma t}{2\pi\eta} \tag{2}$$

where x is the radius of contact between the drops [19]. Compared to the relaxation analysis of free 3D aggregates, 2D aggregates offer some advantages: they are not moving, nor rotating nor flattening on a nearby surface. The 2D system also allows to track simultaneously cell motion.

We previously showed that cell motion consists both of random and coherent components [10] and studied precisely random cell displacements and deformations using confocal microscopy [11]. On the other hand, coherent motion was poorly studied quantitatively. Here we show that during rounding of elongated aggregates, cell motion is strongly cooperative. Neighboring cells exhibit parallel trajectories with both correlations at long times and long distances, and little lateral random fluctuations. When the initial aggregate shape approaches a perfect ellipse, the displacement pattern is very symmetric (Fig. 5b). The average velocity is larger during rounding up of the aggregate than during the period of random motion once aggregate rounded. This is again a clear hint that motion is strongly cooperative during rounding. Phillips and Steinberg suggested from the observation of the shape relaxation of centrifuged aggregates that coherent motion arises when cells are strongly but not irreversibly bound to one another (irreversible bonds prevent relative motion between cells) [7]. Such a "liquid like" cooperative motion is not the only possible correlated cell motion. In simulations of cell aggregates using the Potts model [11,20], we observed that for a large set of parameters investigated, cell motion remains random and uncorrelated within the center of the aggregate at short and intermediate times even in the presence of long time biases due to internal sorting or internal rounding [21]. This different behavior between simulations and our experimental observations is likely due to the presence of adhesive molecules forming tight bonds in real cells [22]. In simulations, bonds are absent, adhesion is modelled as a surface energy proportional to the contact area between neighboring cells. A realistic model of cellular aggregates has thus to take into account these discrete adhesive bonds and their possible diffusion within the cell membrane.

The origin of the observed circular flows is an intriguing issue. Recently, Wu and Libchaber observed swirls and jets in concentrated 2D populations of swimming bacteria [23]. In their system as in our, there are no identifiable temperature or chemical gradient which can drive some instabilities. There are many other possible instability mechanisms [24]. A gradient of cell density around the boundary of the aggregate where cells seem loosely packed after some time, could induce differential adhesion forces able to drive convection. To our best knowledge, this situation was never examined. Also, it is know that self-propelled particles may spontaneously organize, and even create vortexes in circular aggregates, due to the coupling between cell adhesion, cell deformability and exclusion volume [25]. Reduced adhesion prevents the formation these structures in simulations [25]. However, in our case we always observed circular flows in the less cohesive ectodermal aggregates.

Cell-cell adhesion is also responsible for the huge effective tissue viscosity. Taking a reasonable value for the surface tension, *i.e.* $\sigma = 0.3 \sim 10$ mN/m [5,8,18], we indeed obtain a tissue viscosity in the range 10^4 to 3×10^5 Pa s which is 10^6 to 10^8 times higher than water viscosity. Such a high viscosities agree with previous measurements in chicken embryo aggregates [2,8]. Reported viscosities of individual cell differ by nearly three orders of magnitude [26,27]. They depend on cell types, on shear rate [28] and on experimental techniques (intracellular or whole cell measurements [27]). Largest values (*i.e.*, $\eta \simeq 10^4$ Pa s) were measured for individual fibroblast and endothelial cells [26]. The equivalent bulk viscosities of surfactant layers, *i.e.*, $\eta \simeq 150 \sim 2000$ Pa s [16,17], and of phospholipid bilayers *i.e.*, $\eta \simeq 2 \sim 200$ Pa s [29] are also smaller than our estimates. Thus, we believe that in cellular aggregates the high viscosity results from the sliding friction between adjacent cell membranes bonded by adhesive molecules. This friction is higher than the friction experienced between pure lipid bilayers due to the coupling of the adhesive molecule with the cytoskeleton, and also due to membrane ruffles and extracellular matrix [22].

Lastly, quantitative difference between physical parameters of different cell types are discussed. We have measured in this work a ratio $\eta/\sigma \simeq 0.5$ min/μm identical for the three kinds of *hydra* aggregates investigated (ectodermal, endodermal and mixed). Surface tension of *hydra* aggregates was never measured, however from both measurements of adhesion at the level of a single cell pair using optical tweezers [30] and the fact that endodermal cells are surrounded by ectodermal cells at the end of cell sorting, we can reasonably assume that endodermal tissues are the more cohesive (*i.e.* have the larger surface tension). Hence, among the two *hydra* cell types endodermal cells have the higher viscosity. It is also confirmed by the hierarchy of diffusion constants previously measured in *hydra* aggregates: $D_{endo} \simeq 0.5$, $D_{endo} \simeq 1.2$ μm^2/min [11]. Indeed according to the Stoke Einstein's law $D = k_B T/6\pi\eta a$, the diffusion constant of a Brownian particle of radius a is slower in a more viscous medium. Of course, for cell aggregates, one cannot exclude that the effective temperature (which represents the effective temperature of the cellular bath [11,23]) varies according to the cell type [11].

Taking our estimate $\eta \sim 10^4$ Pa s, we obtain the cellular energy $k_BT \sim 10^{-13}$ J. In chicken embryos aggregates, η/σ seems slightly larger (*i.e*, 0.6 $\sim$ 3.8 min/μm [2] and 4.9 min/μm [32] from the fusion of different aggregate types), while the diffusion constant of single pigmented cells in neural cell aggregates is 15 to 30 times smaller than in *hydra* aggregates [31]. It indicates that viscosity is smaller while cellular activity is higher in case of hydra aggregates.

6 Conclusion

In this paper, we have shown that the relaxation of 2D aggregates follows the hydrodynamics laws of viscous liquids. We obtained large estimates of the tissue viscosity comparable to the rare other measurements available. Cell motion is strongly correlated during rounding. It indicates that adhesive molecules in the cell membrane control cell motion as well as the value of physical parameters describing the system (surface tension, viscosity, effective temperature). From the physical point of view, further theoretical work is required to understand the dynamics of such a system of deformable, active and adhesive cells. It would be also interesting to compare 2D and 3D relaxations and to use spacers of different thicknesses in order to find any dependence of tissue viscosity and surface tension on the system dimensionality. From a biological point of view, changes in tissue spreading or cell sorting mediated by differences in the level of expression of adhesive molecules have already been observed qualitatively [33,34], it would be also interesting to measure quantitatively how cell-cell adhesion modifies the value of the physical parameters discussed here.

We would like to thank François Graner, James Glazier, Catherine Barentin and Christophe Ybert for useful discussions. The warm hospitality of Tohoku University is gratefully acknowledged.

References

1. D.A. Beysens, G. Forgacs, J.A. Glazier, Proc. Nat. Acad. Sci. USA. **97**, 9467 (2000).
2. R. Gordon, N.S. Goel, M.S. Steinberg, L.L. Wiseman, J. theor. Biol. **37**, 43 (1972).
3. M.S. Steinberg, Science **141**, 401 (1963).
4. M.S. Steinberg, J. Exp. Zool. **173**, 395 (1970).
5. R.A. Foty, G. Forgacs, C.M. Pfleger, M.S. Steinberg, Phys. Rev. Lett. **72**, 2298 (1994).
6. R.A. Foty, C.M. Pfleger, G. Forgacs, M.S. Steinberg, Development **122**, 1611 (1996).
7. H.M. Phillips, M.S. Steinberg, J. Cell Sci. **30**, 1 (1978).
8. G. Forgacs, R.A. Foty, Y. Shafrir, M.S. Steinberg, Biophys. J. **74**, 2227 (1998).
9. E.K. Mann, S. Hénon, D. Langevin, J. Meunier, L. Léger, Phys. Rev. E **51**, 5708 (1995).
10. J.-P. Rieu, N. Kataoka, Y. Sawada, Phys. Rev. E **57**, 924 (1998).
11. J.-P. Rieu, A. Upadhyaya, J.A. Glazier, N.B. Ouchi, Y. Sawada, Biophys. J. **79**, 1903 (2000).
12. U. Technau, T. Holstein, Dev. Biol. **151**, 117 (1992).
13. A. Gierer, S. Berking, H. Bode, C.N. David, K. Flick, G. Hansmann, H. Schaller, E. Trenkner., Nature New Biol. **239**, 98 (1972).
14. Y. Kishimoto, M. Murate, T. Sugiyama., J. Cell. Sci. **109**, 763 (1996).
15. NIH Image is a public domain program developed at the U.S. National Institutes of Health and available on the Internet at `http://rsb.info.nih.gov/nih-image/`.
16. F. Bouchama, J.-M. di Meglio, Colloid Polym. Sci. **278**, 195 (2000).
17. C. Barentin, C. Ybert, J.-M. di Meglio, J.-F. Joanny, J. Fluid Mech. **397**, 331 (1999).
18. G.S. Davis, H.M. Phillips, M.S. Steinberg, Dev. Biol. **192**, 630 (1997).
19. J. Frenkel, J. Phys. (USSR) **9**, 385 (1945).
20. F. Graner, J.A. Glazier, Phys. Rev. Lett. **69**, 2013 (1992); J.A. Glazier, F. Graner, Phys. Rev. E **47**, 2128 (1993).
21. J.-P. Rieu (unpublished).
22. P. Bongrand, *Physical Basis of Cell-Cell Adhesion* (CRC, Boca Raton, 1988), Chaps. 7 and 10.
23. X.L. Wu, A. Libchaber, Phys. Rev. Lett. **84**, 3017 (2000).
24. P. Manneville, *Dissipative Structures and Weak Turbulence*, edited by H. Araki, A. Libchaber, G. Parisi (Academic Press, San Diego, 1990).
25. W.J. Rappel, A. Nicol, A. Sarkissian, H. Levine, W.F. Loomis, Phys. Rev. Lett. **83**, 1247 (1999).
26. O. Thoumine, A. Ott, J. Cell Sci. **110**, 2109 (1997).
27. S. Yamada, D. Wirtz, S.C. Kuo, Biophys. J. **78**, 1736 (2000).
28. M.A. Tsai, S.R. Franck, R.E. Waugh, Biophys. J. **65**, 2078 (1993).
29. R. Dimova, B. Pouligny, C. Dietrich, Biophys. J. **79**, 340 (2000).
30. M. Sato-Maeda, M. Uchida, F. Graner, H. Tashiro, Dev. Biol. **162**, 77 (1994).
31. J.C. Mombach, J.A. Glazier, Phys. Rev. Lett. **76**, 3032 (1996).
32. A. Upadhyaya, Ph.D. Thesis, University of Notre Dame, USA (2000).
33. M.S. Steinberg, M. Takeichi, Dev. Biol. **91**, 206 (1994).
34. D. Godt, U. Tepass, Nature **395**, 387 (1998).